Journal of Power Sources 195 (2010) 6157–6161

Contents lists available at ScienceDirect

Journal of Power Sources

journal homepage: www.elsevier.com/locate/jpowsour

Short communication

Electrochemical characteristics of lithium vanadate, $Li_{1+x}VO_2$, new anode materials for lithium ion batteries

Jun Ho Song[a], Hye Jung Park[a], Ki Jae Kim[a], Yong Nam Jo[a], Jeom-Soo Kim[a], Yeon Uk Jeong[b], Young Jun Kim[a,*]

[a] Advanced Batteries Research Center, Korea Electronic Technology Institute, Gyeonggi-do 463-816, Republic of Korea
[b] School of Materials Science and Engineering, Kyungpook National University, 1370 Sankyuk-dong, Buk-gu, Daegu 702-701, Republic of Korea

ARTICLE INFO

Article history:
Received 20 October 2009
Received in revised form
22 December 2009
Accepted 22 December 2009
Available online 13 January 2010

Keywords:
Li-ion batteries (LIBs)
Anode material
Lithium vanadate
Transition metal oxide
Ex situ X-ray diffraction
Spray pyrolysis technique

ABSTRACT

Lithium vanadium oxide has been synthesized as an anode material for lithium ion batteries by spray pyrolysis technique. The precursor prepared by spray pyrolysis is sintered at 1000 °C under 10% H_2/Ar atmosphere.

Highly crystallized hexagonal lithium vanadate, $Li_{1+x}VO_2$, is obtained without any impurities. The product has mean particle size of 7–8 μm. Lattice parameters of as-prepared powders vary largely according to Li/V ratio. The powder having the lowest *c*/*a* ratio shows the largest discharge capacity. Optimum *x* value is 0.2 in the view point of the discharge capacity (294 mAh g^{-1}) and the cycle retention (>90%, after 25 cycles).

Structural change of as-prepared lithium vanadate is investigated by ex situ X-ray diffraction analysis on charged electrodes at various state of charge (SOC). Lithium vanadate undergoes two step phase transition during charging process and its main peak gets broader as the charge state gets higher. This peak broadening is explained by the breaking down of particles at high SOC.

1. Introduction

Recently many researchers and manufacturers in lithium ion battery field pay attention to alternative power sources for automobile and energy storage systems for power grids and renewable energy systems [1]. Generally, those applications require higher energy than mobile electronics need. Higher energy applications translate into higher battery capacities. However, as the battery capacity increases safety requirements for battery chemistry quickly become crucial. Therefore, most popular chemistries used in today's mobile electronic devices may not allow scaling up battery dimensions and new, safer chemistries are being sought.

Transition metal oxides have been surveyed for many years as lithium ion battery anode materials. The types of these anode materials are classified into two groups: (1) decomposition compounds, SnO and CoO and (2) insertion or intercalation compounds, typically $Li_4Ti_5O_{12}$, $LiVO_2$. Many researchers have investigated various transition metal oxides having high capacity, typically decomposition compounds [2,3]. These transition metal oxides are candidates for high capacity applications, but exhibit poor capacity retention and rate-capability speculated by large volume change associated with charge/discharge [4].

Meanwhile, insertion compound such as $Li_4Ti_5O_{12}$ has excellent cycling capability but relatively low discharge capacity compared with graphite anode material. Particularly, fairly high discharging voltage characteristic at approximately 1.5 V (vs. Li/Li^+) can improve the battery safety but reduces the cell voltage [5,6].

To overcome these limitations, it is necessary to find the new insertion compound with higher capacity and lower discharge voltage than $Li_4Ti_5O_{12}$. Lithium vanadate has layered structure with hexagonal system and about 260 mAh g^{-1} at first discharge and relatively low discharging voltage profile (<0.4 V vs. Li/Li^+). Moreover lithium vanadate makes a composite easily with commercial graphite anode due to similar voltage characteristics, and then this composite has higher volumetric energy density and better safety of the battery [7]. Previously reported $Li_{1.1}V_{0.9}O_2$ has been synthesized by solid state reaction of lithium carbonate and vanadium (III) oxide [8].

In this study, $Li_{1+x}VO_2$ (x = 0.00–0.35) has been synthesized by spray pyrolysis. The spray pyrolysis technique is very competitive method to prepare intermediate compounds with high homogeneity. Vanadium (V) oxide was selected as a raw material for vanadium source in the view point of cost effectiveness. By applying spray pyrolysis, authors were able to use the high oxidative metal source, Vanadium (V) oxide. The effects of extra lithium (x) in the crystal structure on the structure, the morphology, and the electrochemical characteristics of $Li_{1+x}VO_2$ anode material have been investigated.

* Corresponding author. Tel.: +82 31 789 7490; fax: +82 31 789 7499.
E-mail address: yjkim@keti.re.kr (Y.J. Kim).

0378-7753/$ – see front matter © 2010 Elsevier B.V. All rights reserved.
doi:10.1016/j.jpowsour.2009.12.103

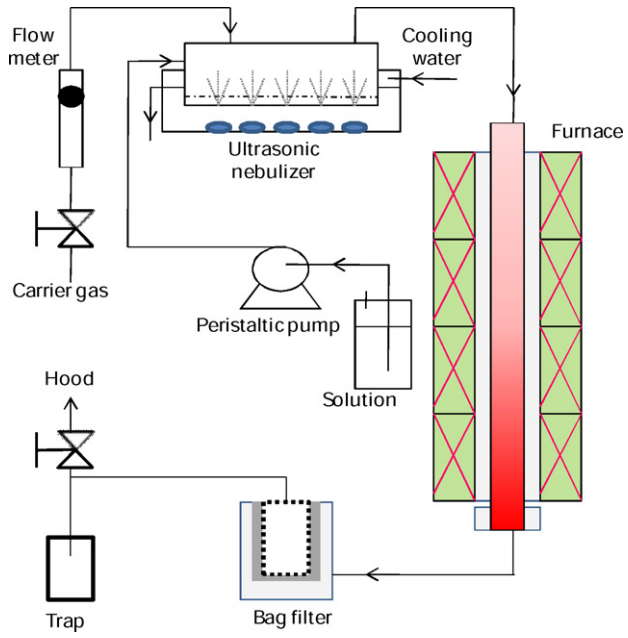

Fig. 1. Spray pyrolysis synthesis diagram of lithium vanadate anode material.

2. Experimental

The experimental setup of spray pyrolysis for Li and V intermediates is presented in Fig. 1. Spray pyrolysis technique is well known for the preparation of homogeneous mixtures or intermediates for starting materials. Vanadium (V) oxide (V_2O_5, Aldrich 99.5%) and lithium hydroxide (LiOH, Aldrich 99%) were used as starting materials. The precursor solution was prepared by dissolving lithium carbonate and vanadium (V) oxide in distilled water. The overall solution concentration of Li, V components was 1 M. This prepared solution was poured into the ultrasonic nebulizer directly in order to create the minute droplets. The bubbled precursor was carried by 10% H_2/Ar gas into the vertical tube furnace at various temperatures, 800–1050 °C. The as-prepared power was obtained by posttreating of precursors at the temperature range of 800–1050 °C for 10 h under 10% H_2/Ar atmosphere.

Powder X-ray diffraction (XRD) patterns were obtained with a D8-Brucker diffractometer equipped with monochromated Cu Kα radiation (1.54056 Å). Powder morphology was characterized by using Field Emission Scanning Electron Microscope (FE-SEM), JEOL JSM-7000 F. The composite anode electrode was prepared by mixing of $Li_{1+x}VO_2$ powder, a carbon additive (Super-P), and poly(vinylidene difluoride) (PVDF) as a binder by 80:10:10 wt. ratio. Mixed slurry was coated on the piece of Cu foil followed by vacuum drying at 80 °C and pressing. 2032 coin-type half cells were fabricated with the composite electrodes. Li foil was used as a counter and reference electrode. The electrolyte solution was 1 M $LiPF_6$ in 3:7 mixture by volume of EC/DEC. Galvanostatic charge/discharge cycling was performed using a TOSCAT 3100 (Toyo) cycler using constant current (CC) mode and constant current/constant voltage (CCCV) mode.

In this paper, lithiation is expressed as charge, whereas delithiation as discharge.

3. Results and discussion

The intermediate precursor prepared by spray pyrolysis has spherical shape and uniform particle size distribution. The mean size of final product $Li_{1+x}VO_2$ (x = 0.00–0.35) powders measured from FE-SEM images were about 5–15 μm. Their morphologies are very similar to layered lithium transition metal oxide, specially $LiCoO_2$, as shown in Fig. 2.

Lithium vanadium oxide has hexagonal structure with successive layers of vanadium, oxygen, and lithium ions. Powder XRD

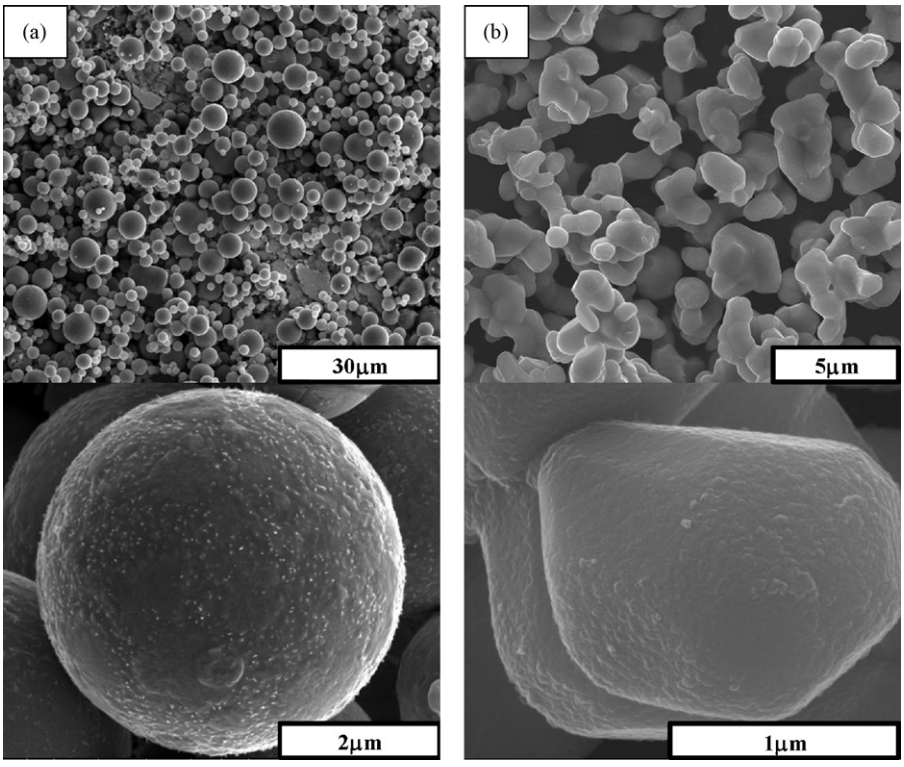

Fig. 2. FE-SEM images of the lithium vanadate powders: (a) lithium vanadate precursor material with spherical morphology by spray-pyrolysis and (b) the prepared lithium vanadate powder at 1000 °C.

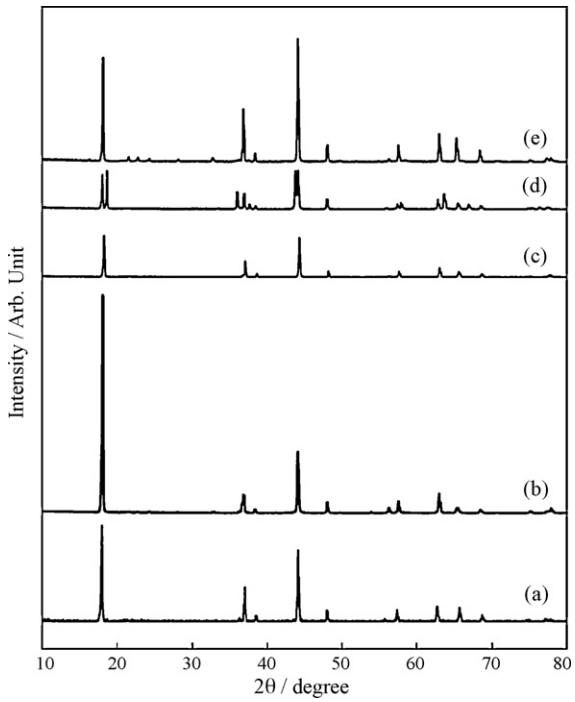

Fig. 3. Powder X-ray diffraction patterns of the prepared $Li_{1+x}VO_2$ powders according to Li/V ratio: (a) 1.00, (b) 1.20, (c) 1.25, (d) 1.30, and (e) 1.35.

patterns of as-prepared anode materials are represented in Fig. 3. Excess Li ions (x) in $Li_{1+x}VO_2$ materials are easily doped into the structure in the range of $0.0 < x < 0.3$ and show high crystalline structure without any other impurities. When the value of x exceeds 0.3, an additional phase starts growing indicated by main peak separation ($2\theta = 17.98, 18.56$) in Fig. 3(d). In case of the highest Li/V ratio ($x = 0.35$), the impurity is identified as a Li_3VO_4 phase shown in Fig. 3(e).

Table 1 shows lattice information and electrochemical properties of various $Li_{1+x}VO_2$ ($0.00 \le x \le 0.35$). While the lattice a increases smoothly as x amount increases, the lattice c decreases initially and then increases in the range of $0.0 < x < 0.25$. The lattice c has a minimum value of 14.69_3 at $x = 0.2$. This behavior is not fully understood currently. One possible postulate is that this structural variation is caused by excess Li ions which exist in distorted tetrahedral Li site and/or in octahedral vanadium site [9]. Further investigation is necessary to clarify this issue.

The relationship between lattice parameter, especially c/a ratio, and the first discharge capacity is represented in Fig. 4. As-prepared $Li_{1.20}VO_2$ with about 5.15 in lowest c/a value level has the highest discharge capacity. It is suggested that excess Li ions up to 20% level enhance the Li intercalation/de-intercalation kinetics at tetrahedral site in the layered structure, but additional Li more than 20% induces less utilization of lithium by decreased electrochemically active Li site at fully charged state, Li_2VO_2.

Table 1
Lattice parameters and electrochemical characteristics of as-prepared $Li_{1+x}VO_2$ ($x = 0.00$–0.35)/Li coin cell during first cycle.

Li/V	Lattice parameter (Å)			1st capacity (mAh g^{-1})	
	a	c	c/a	Discharge (mAh g^{-1})	Efficiency (%)
1.00	2.83_9	14.84_6	5.22_9	32	46
1.05	2.84_1	14.76_6	5.198	92	64
1.15	2.84_8	14.71_8	5.168	232	73
1.20	2.85_3	14.69_3	5.14_8	246	77
1.25	2.85_4	14.72_8	5.16_1	212	70
1.30	2.89_1	14.70_2	5.08_5	128	66
	2.83_1	14.62_6	5.16_7		
1.35	2.85_3	14.69_9	5.15_1	156	61

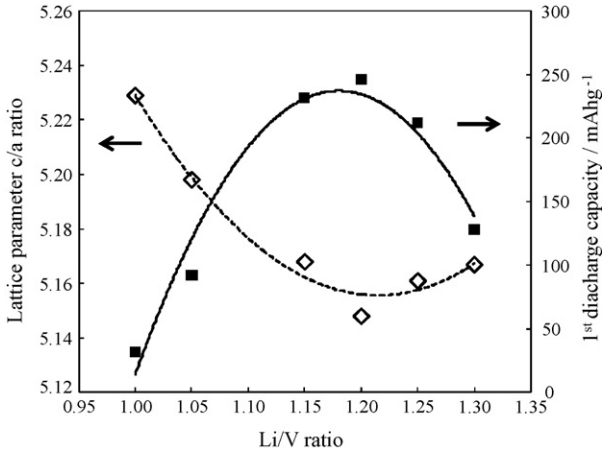

Fig. 4. Relationship between the lattice parameter c/a value of the prepared lithium vanadate powder and first discharge capacity according to Li/V.

Lithium vanadium oxide has very low and flat charge/discharge voltage profiles compared with other metal oxides having insertion reaction characteristic [8]. To elucidate this difference clearly, the differential capacity plot of as-prepared $Li_{1.20}VO_2$ material is shown in Fig. 5. The large redox couple peaks at the first cycle appear in about 0.1 V (vs. Li/Li$^+$) on charging and 0.35 V on discharging. This voltage difference at the first cycle decreases at following second cycle from 0.25 V to 0.11 V.

The irreversible peak is appeared at approximately 0.48 V (vs. Li/Li$^+$) during the first charge and disappeared during following discharge. Kim and co-authors reported that this irreversible plateau is related to formation of SEI layer on the anode surface [8].

Fig. 6 shows typical charge/discharge profiles and the cycle life of as-prepared $Li_{1.20}VO_2$ materials. As-prepared $Li_{1.20}VO_2$ (a) exhibits the typical large reversible potential plateau around 0.1 V (vs. Li/Li$^+$) on charging and 0.3 V on discharging. During the first cycle, discharge capacity of as-prepared $Li_{1.20}VO_2$ is about 294 mAh g^{-1} under CC–CV condition and 246 mAh g^{-1} under CC condition. The capacity retention of as-prepared $Li_{1.20}VO_2$ is quite poor under CC condition; meanwhile it is improved markedly under CC–CV condition as shown in Fig. 6(b). Although its cycling performance is enhanced, charge/discharge coulombic efficiency is very poor and not improved in 25 cycles. This low coulombic efficiency is resulted

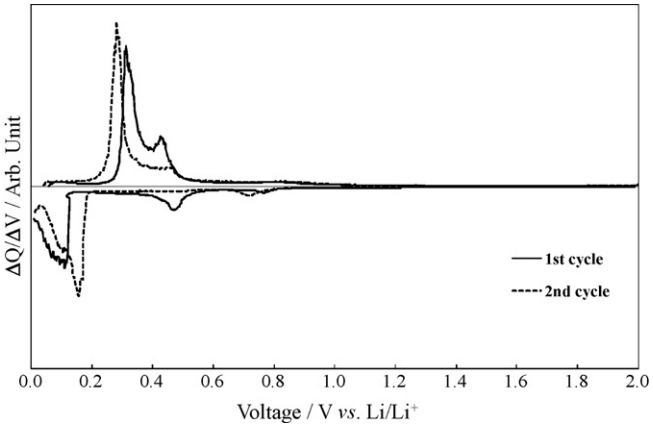

Fig. 5. Differential capacity plot of lithium vanadate/Li cells with potential range of 0.008–2.0 V (vs. Li/Li$^+$) and a current density of 20 mA g^{-1} (0.1 C).

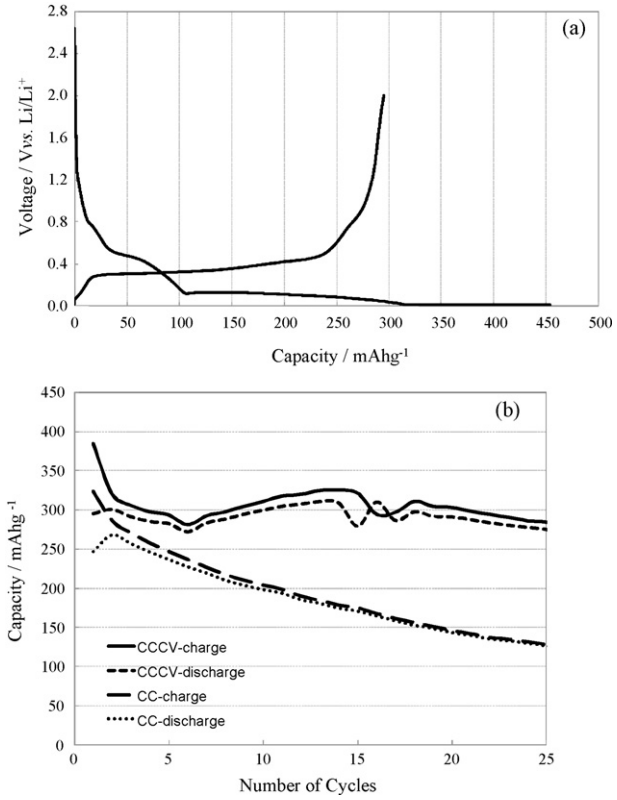

Fig. 6. Electrochemical characteristics of lithium vanadate anode material with 1.20 Li/V ratio: (a) first charge/discharge profiles and (b) cycleability with potential range of 0.008–3.0 V (vs. Li/Li$^+$) and constant current (0.1 C) constant voltage (10% cut-off) (CCCV) condition.

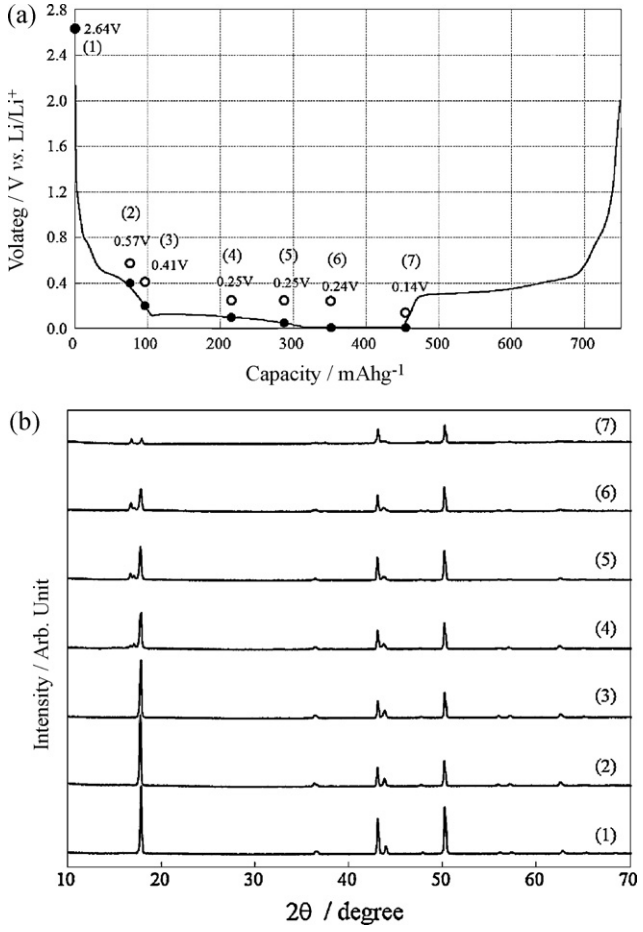

Fig. 8. Structural change of charged lithium vanadate powders according to depth of charge: (a) ex situ X-ray diffraction patterns and (b) ex situ condition and open circuit voltage at each step in first charging profile.

from the side reaction between charged material and electrolyte solution.

Liang's group reported very high discharge capacity of MoO_2 (484 mAh g^{-1}) in the voltage range between 0.008 V and 3.0 V, but charge/discharge efficiency is hardly achieved close to 100% after 13 cycles [10,11]. This result could be explained by "electrochemical grinding" phenomenon that the MoO_2 powder breaks down to the smaller particles in high concentration of Li. As MoO_2 material, $Li_{1.20}VO_2$ powder might break down to the smaller particles in charged state as shown in Fig. 7. This surface change contributes to the cycling efficiency which was not able to reach 100%. Increased surface area causes increased side reaction between electrode and electrolyte solution at charged state.

To confirm "electrochemical grinding" postulate, ex situ XRD analysis of $Li_{1.20+\delta}VO_2$ anode electrode was performed at various depths of charge. Intensity of (0 0 3) main peak in $Li_{1.20+\delta}VO_2$ material diminishes about 1/15 scale from bare material and new peaks appear when the electrode is charged down to 0.1 V (vs. Li/Li$^+$) as shown in Fig. 8. The original main peak and other two new peaks are assigned to hexagonal system with $2\theta = 17.8^\circ$ (phase I), 17.2° (phase II), 16.8° (phase III). From theoretical calculation, volumetric change from phase I to III is about 25.5% [8]. The relationship between main XRD peak variation and powder morphology in charged electrode is shown in Fig. 9. Particle size of as-prepared $Li_{1.20}VO_2$ (Fig. 9(b)) is around 5–15 μm. The morphologies of charged electrodes (Fig. 9(c) and (d)) are quite different from bare-electrode (Fig. 9(b)) those morphologies look quite similar to the diagram shown in Fig. 7.

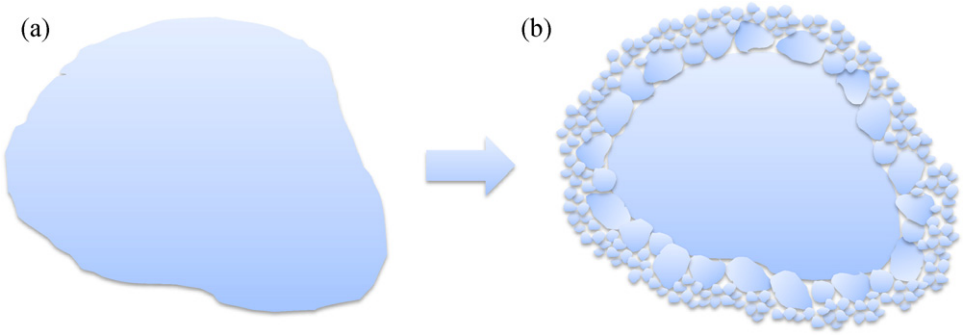

Fig. 7. Conceptional diagram of the morphology change in Lithium vanadate particle during Li intercalation process: (a) fresh $Li_{1.20}VO_2$ particle and (b) Li-intercalated $Li_{1.20+\delta}VO_2$.

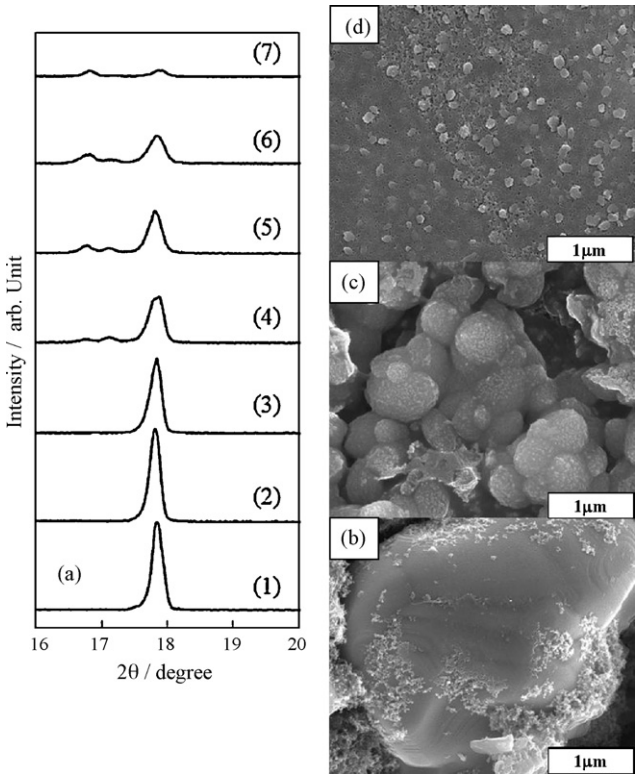

Fig. 9. Relationship between the structural changes of charged lithium vanadate and FESEM images of the charged electrode: (a) main peak split and change in ex situ X-ray diffraction patterns, (b) fresh electrode with notation (1), (c) charged electrode with notation (4), and (d) charged electrode with notation (6).

Dahn et al. reported the structural changes of layered $Li_{1+y}NiO_2$ ($y > 0$) by in situ XRD analysis [12]. During a constant current discharge the Bragg peaks of $LiNiO_2$ phase did not shift in angle, but decreases in intensity while peaks from a new phase appeared and grew. $Li_{1.2+y}VO_2$ ($y > 0$) shows similar structural changes as $Li_{1+y}NiO_2$ ($y > 0$) during lithium intercalation into the structure.

Large volume expansion of $Li_{1+x}VO_2$ induces particle fracture during Li intercalation into the structure. Smaller particles created by this electrochemical grinding may enhance Li ion diffusion as well as capacity utilization. But the coulombic efficiency is decreased because of the side reaction. Proper control of surface area is critical to commercialize $Li_{1+x}VO_2$.

4. Conclusion

$Li_{1+x}VO_2$ ($x = 0.00$–0.35) anode materials having high crystallinity and micron-sized primary particles were successfully synthesized by using the spray pyrolysis technique followed sintering at 1000 °C under 10% Ar balanced H_2 atmosphere. The $Li_{1.20}VO_2$ product shows reversible discharge capacity of 294 mAh g^{-1} at 0.1 C at the first cycle and good capacity retention of 90% after 25 cycles. The phase transition is observed during the Li intercalation of $Li_{1.20}VO_2$. This series of phase changes affects the volume expansion which causes electrochemical grinding. Small particles and large surface area generated by "electrochemical grinding" enhance the diffusion of Li ion as well as the capacity utilization in early stage of cycle. These results suggest that lithium vanadate can be considered as an alternative anode material for lithium ion batteries with proper control of surface morphology.

Acknowledgement

This work was performed in the R&D program "Development of Anode Materials for kWh-grade Energy Storage" by financial support from Ministry of Knowledge Economy.

References

[1] N. Terada, T. Yanagi, S. Arai, M. Yoshikawa, K. Ohta, N. Nakajima, A. Yanai, N. Arai, Journal of Power Sources 100 (2001) 80–92.
[2] H. Li, X. Huang, L. Chen, Solid State Ionics 123 (1999) 189–197.
[3] P. Poizot, S. Laruelle, S. Grugeon, L. Dupont, J.-M. Tarascon, Nature 407 (2000) 496–499.
[4] P. Poizot, S. Laruelle, S. Grugeon, L. Dupont, J.-M. Tarascon, Journal of Power Sources 97–98 (2001) 235–239.
[5] X.L. Yao, S. Xie, C.H. Chen, Q.S. Wang, J.H. Sun, Y.L. Li, S.X. Lu, Electrochimica Acta 50 (2005) 4076–4081.
[6] S.H. Ju, Y.C. Kang, Journal of Power Sources 189 (2009) 185–190.
[7] S.S. Kim, N. Sato, Proceedings of the 8th Advanced Automotive Batteries Conference (AABC), vol. 10, FL, USA, May 13–15, 2008 (Abs.).
[8] N.S. Choi, J.S. Kim, R.Z. Yin, S.S. Kim, Materials Chemistry and Physics 116 (2009) 603–606.
[9] R.Z. Yin, Y.S. Kim, W.U. Choi, S.S. Kim, H.J. Kim, Advances in Quantum Chemistry 54 (2008) 23–33.
[10] Y. Liang, S. Yang, Z. Yi, X. Lei, J. Sun, Y. Zhou, Materials Science and Engineering B 121 (2005) 152–155.
[11] Y. Pihhard, F. Leroux, D. Guyomard, Journal of Power Sources 68 (1997) 698–703.
[12] J.R. Dahn, U.V. Sacken, C.A. Michal, Solid State Ionics 44 (1990) 87–97.